Isovector soft dipole mode in ^{6}Be

M.S. Golovkov[a], I.A. Egorova[b], L.V. Grigorenko[a,c,d], V. Chudoba[a,e], S.N. Ershov[b], A.S. Fomichev[a], A.V. Gorshkov[a], V.A. Gorshkov[a], G. Kaminski[a,f] S.A. Krupko[a], I.G. Mukha[c], Yu.L. Parfenova[a,g], S.I. Sidorchuk[a], R.S. Slepnev[a], S.V. Stepantsov[a], G.M. Ter-Akopian[a], R. Wolski[a,f], M.V. Zhukov[h]

[a]Flerov Laboratory of Nuclear Reactions, JINR, Dubna, RU-141980 Russia
[b]Bogolyubov Laboratory of Theoretical Physics, JINR, Dubna, RU-141980 Russia
[c]GSI Helmholtzzentrum für Schwerionenforschung, Planckstraße 1, D-64291 Darmstadt, Germany
[d]Russian Research Center "The Kurchatov Institute", Kurchatov sq. 1, RU-123182 Moscow, Russia
[e]Institute of Physics, Silesian University in Opava, Bezručovo nám. 13, 74601 Czech Republic
[f]Institute of Nuclear Physics PAN, Radzikowskiego 152, PL-31342 Kraków, Poland
[g]Skobeltsyn Institute of Nuclear Physics, Moscow State University, 119991 Moscow, Russia
[h]Fundamental Physics, Chalmers University of Technology, S-41296 Göteborg, Sweden

ABSTRACT

Continuum ^{6}Be states up to $E_T = 16$ MeV were populated in the $p(^6$Li,^{6}Be$)n$ charge-exchange reaction (the energy E_T is considered from the three-body $\alpha+p+p$ threshold). High statistics energy spectrum of ^{6}Be ($\sim 10^7$ events) was obtained in the kinematically complete measurements by detecting $\alpha+p+p$ coincidences. The detailed correlation information about the well-known ^{6}Be 0^+ ground state at $E_T = 1.37$ MeV and the 2^+ state at $E_T = 3.05$ MeV was obtained. A broad structure extending from 4 to 16 MeV contains negative parity states, populated by $\Delta L = 1$ angular momentum transfer, without other significant contributions. This continuum structure can be interpreted as a novel phenomenon: the isovector soft dipole mode associated with the ^{6}Li ground state. The population of this mode in the charge-exchange reaction is a major phenomenon for the involved systems: it is responsible for about 60% of the cross section obtained in the measured energy range.

1. Introduction

Important instrument for studies of the light exotic (halo) nuclei is electromagnetic excitation. The existence of a novel dipole mode at low excitation energies was predicted in Ref. [1, 2, 3], based on the halo hypothesis. This so-called soft dipole mode (SDM) [or soft mode of the giant dipole resonance (GDR)] is related to the low binding energy of the halo nucleon(s). It allows low-frequency oscillations of the halo nucleon(s) against the core creating the low-lying dipole excitations and providing abnormally large low-energy electromagnetic dissociation cross sections. The experimental studies confirmed these expectations [4, and Refs. therein] and showed that the observed low-lying E1 strength is in a good agreement with the cluster non-energy-weighted sum rule.

The ^{6}Be system is an isobaric partner of the "classical" halo nucleus ^{6}He and there are several issues of special interest here. The ground state (g.s.) of ^{6}Be is particle unstable. This nucleus is the lightest ground-state *true two-proton* ($2p$) emitter. True $2p$ emission is a genuine quantum-mechanical phenomenon: a pairing effect can cause the energy conditions in unbound even systems, which makes emission of one proton prohibited while two protons should be emitted simultaneously. The specific correlation patterns in the decay of ^{6}Be inspired the concept of *democratic decay* [5], which has now become generally accepted. In heavier $2p$ unstable nuclei a true $2p$ emission is arising in

the form of *two proton radioactivity* [6]. Comparative correlation studies of ^{6}Be vs. ^{45}Fe presenting this short-living system in the context of $2p$ radioactivity are performed in Ref. [7]. Enormous efforts have been invested in the studies of the halo aspect of the ^{6}He structure in the last two decades. Recently it has been demonstrated in Ref. [8] that a valuable alternative to studies of the ^{6}He g.s. itself could be precision studies of the correlations in the decay of the particle-unstable ^{6}Be ground state.

In our work the ^{6}Be spectrum was studied in the charge-exchange $p(^6\text{Li},^6\text{Be})n$ reaction. We identified properties of the ^{6}Be continuum above the last well-established state (2^+ at $E_T = 3.03$ MeV). We found that this continuum is represented exclusively by negative parity states (populated by $\Delta L = 1$ transitions) in the broad energy range (up to about 16 MeV). The negative parity continuum in ^{6}Be can be seen analogous to the soft dipole mode in ^{6}He. Based on the $\Delta L = 1$ identification in the charge exchange reactions with ^{6}Li, it was suggested that the low-energy continuum properties of ^{6}He [9, 10, 11] and ^{6}Be [12] may have character of some form of soft dipole excitation. In this work we state it with the confidence and considerably clarify the issue basing on the correlation information. The obtained results brings qualitatively new insight on this question. We also point to important differences of our results with the SDM in ^{6}He, which enables us to speculate about a novel phenomenon: an isovector breed of soft dipole mode (IVSDM). Having in mind the interest attracted by SDM in exotic (dripline halo) nuclei as a tool for nuclear-structure and nuclear-astrophysics studies, we dedicate this Letter to prove the existence of such a new phenomenon.

2. Experiment

A 47 A MeV ^{6}Li beam was produced at the U-400M cyclotron of the Flerov laboratory at JINR (Dubna, Russia [13]). The projectile energy 32.5 A MeV was defined by carbon degrader and ACCULINNA fragment separator [14] which served for beam transport to the reaction chamber and monochromatization. As a result the beam sport of 6 mm diameter was obtained on the cryogenic hydrogen target with intensity of about 3×10^7 s^{-1} and an energy spread better than 0.5%. The cryogenic cell was 6 mm thick, enclosed with 20 mm diameter, 6 μm thick stainless-steel windows. Working pressure and temperature were 3 bar and 35 K, respectively. Reaction products were measured by two identical annular telescopes placed 91 and 300 mm downstream the target. Each telescope consisted of two position-sensitive silicon detectors (300 and 1000 μm thick) and an array of 16 trapezoid CsI(Tl) crystals with a PIN-diode readout. The inner and outer diameters of the active zone of silicon detectors were 32 and 82 mm. The first detector was segmented in 32 rings on one side and 32 sectors on the other. The second silicon detector was segmented in 16 sectors. CsI(Tl) crystals were 19 mm thick with the inner and outer diameters of the assembly of 37 and 90 mm. Angular ranges of the first and the second telescopes were $\sim 3 - 8°$ and $\sim 10 - 24°$, respectively. Each segment of the telescopes had an independent acquisition channel, which allowed registration of coincidence events
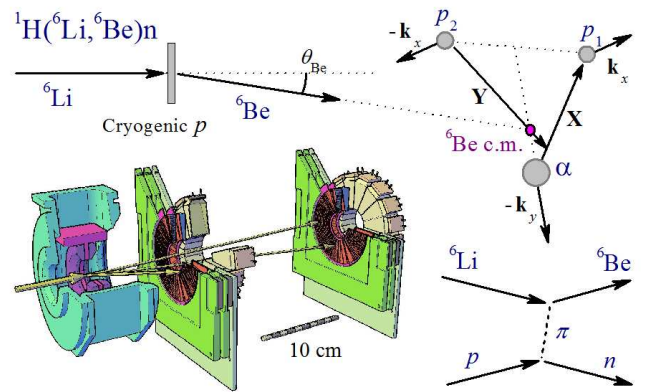

Fig. 1. Experimental setup and kinematical diagram. Coordinate space Jacobi variables **X** and **Y** are shown for "Y" system, as used in Eq. (5). Momentum space Jacobi variables $\mathbf{k}_x$ and $\mathbf{k}_y$ are shown for "T" system, as used in Eq. (6).

caused by several simultaneous hits. Particle identification was provided by the standard ΔE-E method. Schematic view of the setup, the kinematical diagram, and kinematical variables are shown in Fig. 1. It should be noted that very high statistics ($\sim 10^7$ $2p$-decay events) were obtained in our experiment.

3. Energy spectrum of ^{6}Be

The current analysis deals only with those events which correspond to triple $p+p+\alpha$ coincidences. The invariant-mass spectrum of ^{6}Be was reconstructed together with a momentum of center of mass (c.m.) motion of ^{6}Be in laboratory system. Due to inverse kinematics for the ^{1}H(^{6}Li,^{6}Be)n reaction, the ^{6}Be decay products fly out in a narrow angular cone relative to the beam direction. Therefore, the experimental setup allows the registration with reasonable efficiency of the ^{6}Be decays almost in whole angular range up to 15 MeV of ^{6}Be excitation energy. In Fig. 2 (a) the ^{6}Be invariant-mass spectrum measured in the whole angular range is presented. The 0^+ ground state at $E_T = 1.37$ MeV and the 2^+ first excited state at $E_T = 3.05$ MeV are undoubtfully identified directly in the inclusive spectrum. The width of the g.s. peak demonstrates the overall instrumental energy resolution of the experiment. In the measured spectrum, these two peaks are superimposed on the broad hump which starts practically from the energy of the ground state and has a maximum at $E_T \sim 6 - 7$ MeV. The right-hand slope of the hump is due to the decrease of the registration efficiency which is governed by two main factors: (i) the upper limit of the angular acceptance (the ^{6}Be decay products fly out in a wider cone) and (ii) the upper energy threshold of the proton registration (with the rise of the excitation energy the proton energy distribution becomes broader and the protons with energy more then 45 MeV are not detected by the first 300 μm detector). In the Fig. 2 (c), the same spectrum is shown as a two dimensional plot E_T vs. θ_{Be} [the latter is the ^{6}Be c.m. angle for the ^{1}H(^{6}Li,^{6}Be)n reaction]. It should be noted that the broad hump is characterized by a regular behavior in whole angular range. It will be shown below that the structure

shows similar regularity both in angular distribution and in distributions of kinematical variables for three-body decay.

Population of the ^{6}Be ground state in charge exchange-reaction corresponds mainly to the $\Delta L = 0$ orbital angular momentum transfer, providing a maximum of the cross section at zero degree. In the experimental spectrum Fig. 2 (c), this maximum is suppressed by the low efficiency due to the central hole of the first telescope, see Fig. 1. The central hole of the detector array affects considerably only the low energy part of the ^{6}Be spectrum at forward angle and has no significant influence on the spectrum shape at higher energies. The maximum in the angular distribution for the population of 2^+ excited state (which mainly corresponds to the $\Delta L = 2$ angular momentum transfer) is clearly seen in the region of $\theta_{\text{Be}} = 50 - 70°$. From Fig. 2 (c) one can see that the maximum cross section of the hump at about $35°$ in c.m. system is well below the maximum for population of the 2^+ state situated at about $60°$. It is natural to suppose that this whole structure is related to the $\Delta L = 1$ angular momentum transfer, populating possible $J^- = \{0^-, 1^-, 2^-\}$ configurations. To extract quantitative information about properties of this phenomenon, the experimental distortions due to geometry of the detector system and the efficiency of particle registrations must be taken into account. It can be performed by the Monte-Carlo (MC) simulations if theoretical model for reaction is given.

4. Theoretical model.

To elucidate the basic qualitative aspects of the phenomenon, we have performed theoretical studies extending the experience of Ref. [8]. The properties of the ^{6}Be continuum are studied by constructing the three-body $\alpha + N + N$ wave function (WF) with outgoing asymptotics

$$(\hat{H}_3 - E_T)\Psi_3^{JM(+)} = \hat{\mathcal{O}}\Psi_{\text{gs}}^{J'M'}. \qquad (1)$$

The SDM 1^- continuum in ^{6}He is populated in electromagnetic transitions by

$$\Psi_{\text{gs}} \to \Psi_{^6\text{He}}, \quad \hat{\mathcal{O}} \sim \sum_i Z_i r_i Y_{1m}(\hat{\mathbf{r}}_i), \qquad (2)$$

where index i numbers constituents, which are α-core and two valence nucleons. For population of the low-lying states in ^{6}He and ^{6}Be in the charge-exchange reaction, the general form of transition operator is given by

$$\Psi_{\text{gs}} \to \Psi_{^6\text{Li}}, \quad \hat{\mathcal{O}} \sim \sum_i f_l(q, r_i) \left[\alpha + \beta\sigma_\mu^{(i)}\right] \tau_\pm^{(i)} Y_{lm}(\hat{\mathbf{r}}_i), \qquad (3)$$

where index i numbers two valence nucleons. Operators τ_- and τ_+ populate ^{6}Be and ^{6}He spectra, respectively. Using the effective spin-spin charge-exchange interaction between projectile and target nucleons

$$V(r) = V_0(\sigma^{(1)} \cdot \sigma^{(2)})(\tau^{(1)} \cdot \tau^{(2)}) \exp[-(r/r_0)^2],$$

it can be obtained in the plane wave impulse approximation (PWIA) that

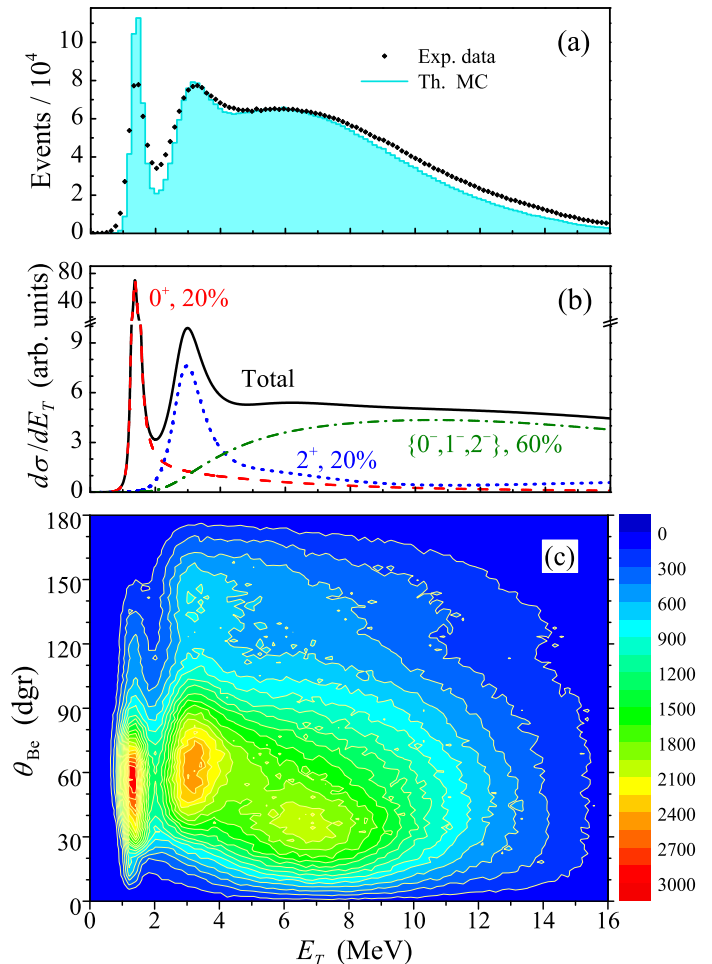$$f_l(q, r_i) = V_0 r_0^3 \sqrt{2}\, \pi^2 \exp[-(qr_0/2)^2]\, j_l(qr_i).$$

Fig. 2. Experimental energy spectrum of ^{6}Be (diamonds) and MC simulation (cyan filled histogram) (a). The energy bin size is 140 keV. Theoretical input for MC simulation (b). Contour plot of the spectrum in the $\{E_T, \theta_{\text{Be}}\}$ plane (c).

Such a simple choice allows to reproduce qualitatively well the angular distributions for ^{6}Be.

We used in the calculations the g.s. WFs Ψ_{gs} provided by the three-body cluster model [15] developed for the $A = 6$ isobar. For the resonant 0^+ and 2^+ states the same method was used which was successfully applied to studies of the 0^+ state in [7]. The calculated cross section profiles are shown in Fig. 2 (b).

The continuum WF of negative parity states were obtained using the Green's function (GF) method [16]

$$\Psi_3^{JM(+)} = \hat{G}_{3E_T}^{(+)} \hat{\mathcal{O}} \Psi_{\text{gs}}^{J'M'}, \qquad (4)$$

where the exact GF of a simplified three-body Hamiltonian is available in compact analytical form

$$\hat{G}_{3E}^{(+)}(\mathbf{XY}, \mathbf{X'Y'}) = \frac{1}{2\pi i} \int_0^E d\varepsilon\, \hat{G}_\varepsilon^{(+)}(\mathbf{X}, \mathbf{X'})\hat{G}_{E-\varepsilon}^{(+)}(\mathbf{Y}, \mathbf{Y'}). \qquad (5)$$

Vectors $\mathbf{X}$ and $\mathbf{Y}$ are Jacobi variables, $\mathbf{X}$ connects core and one of the valence nucleons, $\mathbf{Y}$ connects the second nucleon and c.m. of the remnant. The operator $\hat{G}_E^{(+)}$ is an ordinary two-body GF. This method takes into account one (out of three present) final-state interactions (FSI) exactly. This

was shown to be a good approximation in the case of SDM [16, 17], where the dynamics is defined predominantly by one resonant subsystem (for A=6 nuclei this is evidently the $p_{3/2}$ resonance in α-N subsystem). Analogous approximation has been used in Ref. [18] for SDM studies in ^{11}Li.

Figure 3 (a) shows the comparison of the strength functions for the isoscalar soft dipole mode in ^{6}He [Eq. (2)] and the isovector SDMs [Eq. (3)] in ^{6}He and ^{6}Be built on ^{6}Li. It can be seen that the IVSDMs in ^{6}He for small q values have peak positions close to the isoscalar one, but isovector peaks are much broader. This is an expected consequence of the more compact WF of the ^{6}Li g.s. compared to ^{6}He. However, the steep rise of the spectra occurs in the ^{6}He isovector case at energy comparable with the isoscalar case. When we move across the isobar from ^{6}He to ^{6}Be, Fig. 3 (b), the left slopes of isovector SDMs appear to be in the range of $2-4$ MeV. For IVSDM we demonstrate calculations with $q = 150$ MeV/c ("short wave" case) $q = 100$ MeV/c (typical momentum transfer) and $q = 0.1$ MeV/c (which can be seen as a "long-wave limit"). In the latter case the transition operator behaves like $\sim r_i$ providing dynamical analogue of isoscalar SDM calculations. The long-wave and short-wave responses have quite different shapes. However, the phenomenon is stable to model assumptions about the shape of source term in the sense that the strength functions rise practically at the same energy. One can see that the IVSDM spectra can provide considerable contribution already at 2^+ state energy (around 3 MeV).

Figure 3 (c) shows population of different J^- states in our model. The population of 2^- and 1^- dominates and the contribution of 0^- is minor. Presence of states with negative parity but different J values on one hand makes the picture more complicated than in the case of soft dipole mode in ^{6}He, where only $J^\pi = 1^-$ state is believed to be populated in the Coulomb dissociation. On the other hand, the IVSDM provides access to a wider range of dynamical phenomena, which can be considered as important feature of such studies.

5. Correlations for decay products in ^{6}Be

Internal correlations for states in ^{6}Be in system where nucleus is at rest are shown in Fig. 4. The complete momentum correlations (neglecting initial orientation) for the three-body decay at given decay energy can be described in terms of the energy distribution parameter ε and the angle θ_k between the Jacobi momenta $\mathbf{k}_x$, $\mathbf{k}_y$:

$$\varepsilon = E_x/E_T \quad , \quad \cos(\theta_k) = (\mathbf{k}_x \cdot \mathbf{k}_y)/(k_x\, k_y),$$
$$E_T = E_x + E_y = k_x^2/2M_x + k_y^2/2M_y,$$
$$\mathbf{k}_x = \frac{A_2\mathbf{k}_1 - A_1\mathbf{k}_2}{A_1 + A_2}, \quad \mathbf{k}_y = \frac{A_3(\mathbf{k}_1 + \mathbf{k}_2) - (A_1 + A_2)\mathbf{k}_3}{A_1 + A_2 + A_3}, \quad (6)$$

where M_x and M_y are the reduced masses of the X and Y subsystems (see, e.g. [8] for details).

The correlations for 0^+ state have been studied in papers [7, 8] in details. In these works, the experimental correlation picture was found to be in a very good agreement with the theoretical calculations providing $\chi^2/\nu \sim 1.15 - 1.3$. Comparing our data with the same model calculations for
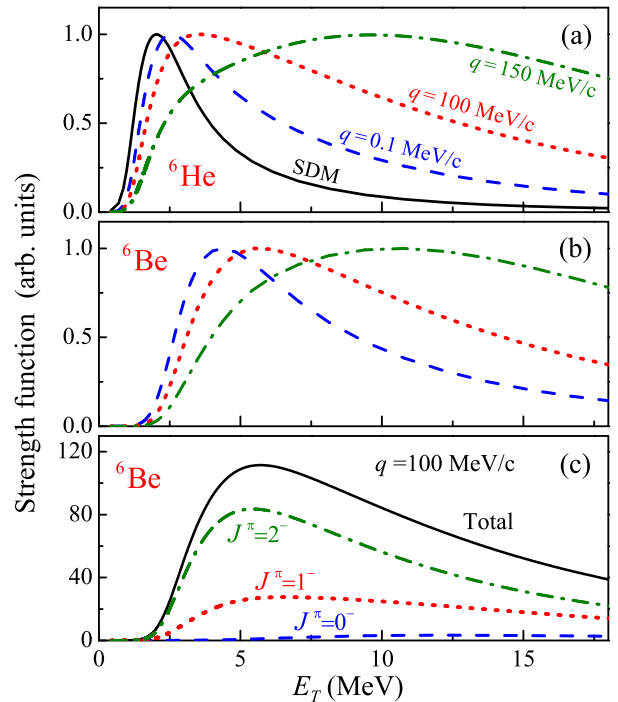

Fig. 3. Theoretical results for negative parity states. (a) SDM (dB_{E1}/dE_T value) and IVSDM ($d\sigma/dE_T$ value) spectra in ^{6}He for different transferred momenta q. (b) IVSDM ($d\sigma/dE_T$ value) spectra in ^{6}Be. Meaning of the curves is the same as in panel (a). Panel (c) shows contribution of different J values to IVSDM spectrum of ^{6}Be. All curves are normalized to unity maximum value.

0^+ and 2^+ states, we find near perfect agreement with theoretical calculations and a low level of distortions introduced by experimental setup, see Fig. 4, columns 1 and 2. This means that the obtained experimental correlation data for the 0^+ state are in agreement with the data from Ref. [8]. High quality complete correlation data for 2^+ state of ^{6}Be are obtained in this work for the first time. Attention should be paid to the qualitative change in the distributions: compared to the 0^+ state, the angular distribution for the 2^+ state is much narrower and peak in the ε is strongly shifted.

When one turns to correlations for broad structure above 2^+ state, on the one hand, a strong qualitative difference with distributions for 0^+ and 2^+ states is seen. On the other hand, the picture for (presumably) J^- states is stable and has certain systematic evolution with energy. The pronounced crescent-like ridges are connected to the ^{5}Li g.s. FSI with fixed $E_T = 2.02$ MeV. The evolution of these ridges is well described under assumption of IVSDM. For the predicted populations of 0^-, 1^-, and 2^- states, our model does not leave place for some uncorrelated phase-volume like contributions in the whole energy range, where the broad structure is observed (4-16 MeV).

6. Angular distributions for the ^{6}Be states

Basing on the predicted energy profiles and internal correlations for different ^{6}Be states, the angular distributions of the ^{6}Be states populated in our experiment can be reconstructed, see Fig. 5 (a). The obtained angular distribution for the ^{6}Be g.s. is in a good agreement with ^{6}Li(p,n) data [19] obtained at very close energy (proton beam at
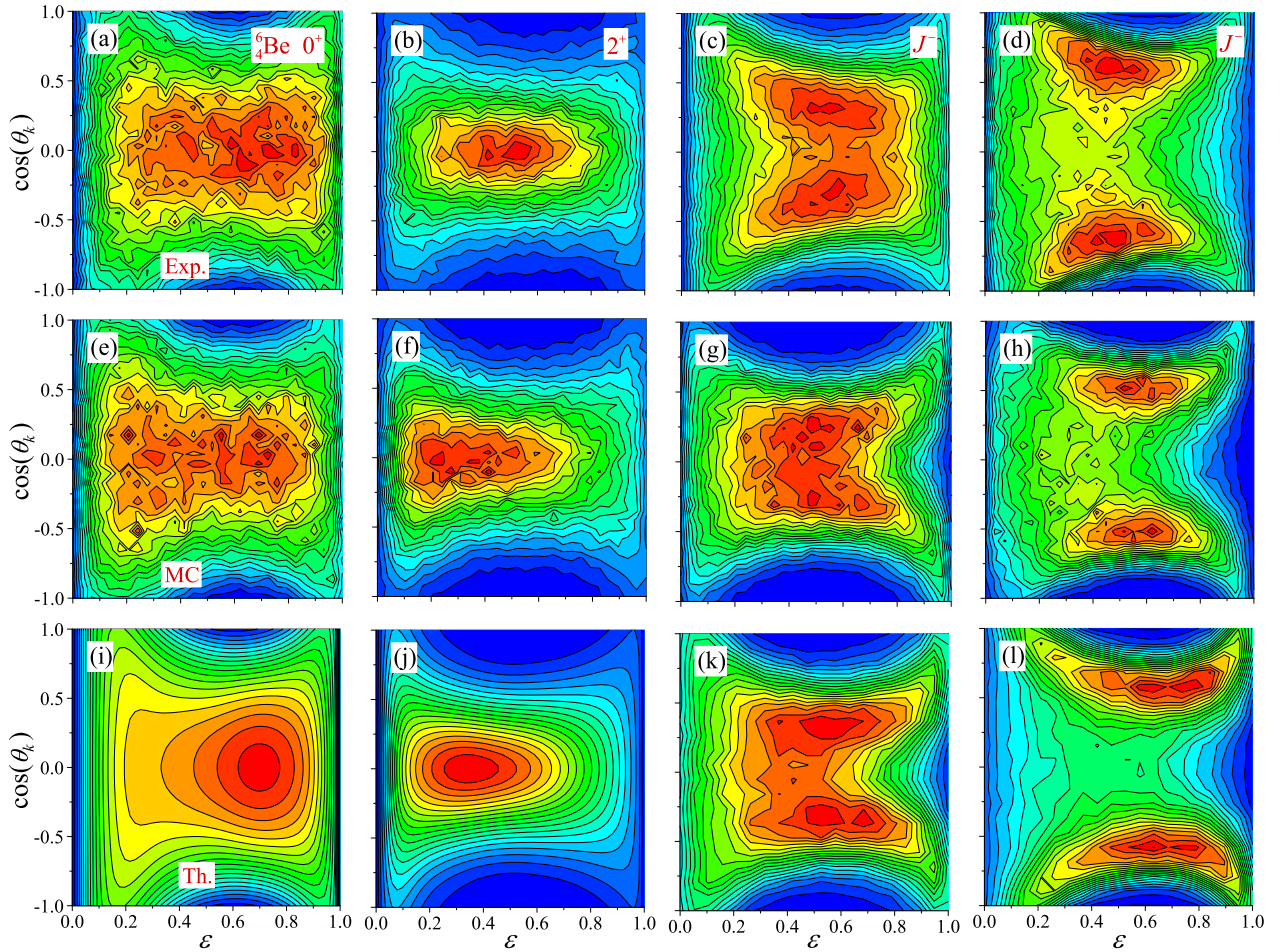
Fig. 4. Comparison of experimental (upper row), MC (middle row), and theoretical (lower row) complete momentum distributions for 0+ (a,e,i), 2^+ (b,f,j) states of ^{6}Be. Comparison for IVSDM J^- configurations in ^{6}Be is provided for energy ranges $5 - 7$ MeV (c,g,k) and $9 - 11$ MeV (d,h,l). Jacobi "T" system. Kinematical variables are defined in Eq. (6).

30.2 MeV). To calibrate the PWIA calculations we used the ^{6}Li(p,n) data from [20]. The transferred momentum distributions obtained for several incident proton energies are reproduced very well with the choice of parameter $r_0 = 0.33$ fm, see Fig. 5 (b). Calculations with such a choice also well reproduce the peak positions of different components of ^{6}Be spectrum, see Fig. 5 (a).

The PWIA calculations indicate that populations of 0^+ and 2^+ are associated mainly with $\Delta L = 0$ and $\Delta L = 2$ transitions, respectively. The 2^+ state also has important contribution from $\Delta L = 0$ which is responsible for rise of the cross section close to forward direction. The broad hump at $E_T > 4$ MeV is easily associated with $\Delta L = 1$. Qualitatively the theoretical distributions are very similar to the experimental ones but quantitatively they do not reproduce the broad components of the angular distributions. These shortage of theoretical descriptions is evidently connected to our simplified treatment of the reaction mechanism, see the discussion of calculations in [19, 21]. It is not expected that this deficiency of our calculations may affect conclusions based on the correlation information. The simple systematics of angular distributions with ΔL and reasonable description of the data by simple PWIA calculations provide strong support for direct reaction mechanism in our experiment and overall consistency of the obtained results.
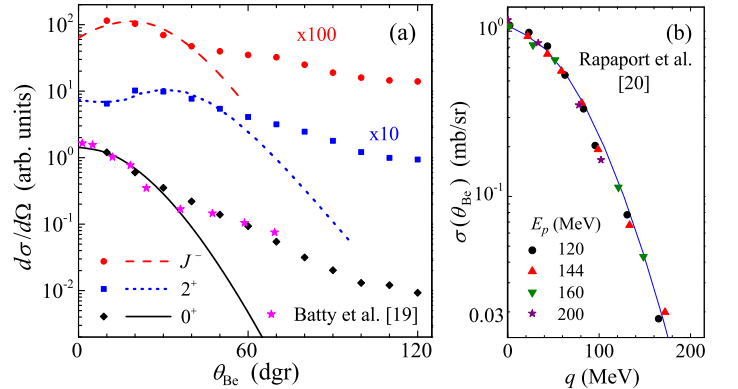

Fig. 5. Angular distributions for states with different J^π (a). Symbols shows the data and curves of the same color provides PWIA results. The resonant 0^+ and 2^+ results are shown on resonance, while IVSDM J^- distribution is integrated over energy. Data of Ref. [19] for the ^{6}Be g.s. is shown for comparison (pink stars). Panel (b) shows g.s. cross section dependence on transferred momentum from Ref. [20] for different proton energies E_p.

7. Theoretical discussion

There is such a wide-spread opinion that the soft dipole mode in the $2n$ halo nuclei is connected to radially extended

ground state *only*. In contrast the calculations demonstrate that effects of the final state interactions are also very important to explain the actually observed soft dipole responses. A proper account for FSI is a challenge for theoreticians. It seems that so far the soft E1 mode in neutron rich nuclei is not completely understood theoretically: there is a systematic disagreement between different calculations [22, 23, 24]. To avoid all the complexities we use simplified, but reliable theoretical model for calculations of soft responses, which provide the major features of the phenomenon. In these conditions, an additional experimental information about soft dipole mode obtained in isovector sector may be indispensable.

The ^{6}Be g.s. is nuclear-unstable and, thus, the strong population of the negative parity continuum can not be interpreted as taking place due to soft excitations based on the weakly-bound and therefore radially-extended ground state. We interpret the observed phenomenon as having two roots: (i) radially extended ground state of ^{6}Li (not that large as in ^{6}He, but still impressive) and (ii) FSI in the negative parity continuum of ^{6}Be.

Exclusive qualitative features of the observed phenomenon are as follows:

(i) Population of ordinary (isoscalar) SDM is not possible in ^{6}Li. In $N = Z$ nuclei the dipole transitions are strongly (say, by 3 orders of the magnitude) suppressed due to effective dipole charges of the nucleons tending to zero. In simple terms, for $N = Z$ systems the centers of neutron and proton distributions coincide making the dipole susceptibility very small.

(ii) Electromagnetic isovector dipole transitions in ^{6}Li (e.g. Ref. [25]) are populated by spin-scalar operator, while in the strong isovector transitions the spin-vector part of the transition is expected to be dominating. These are parts with coefficients α and β respectively in Eq. (3). The above operators populate very different configurations in the final state.

(iii) The isovector soft dipole mode is expected to be sensitive to somewhat different aspect of nuclear structure than the isoscalar soft dipole mode. In ^{6}He, the soft E1 transition to continuum takes place due to interaction with the charged core *only*. In our case, the charge-exchange reaction occurs with the valence nucleons *only*.

(iv) It the case of IVSDM, the opportunity to test isobaric symmetry concept for this class of phenomenon arise, see comparison of Fig. 3. This should be done, of course, in mirror reaction and at the same energy. According to calculations, the IVSDM is "threshold-oriented" phenomenon: one can easily see the Coulomb effect in the *threshold-energy* dependence of Fig. 3 where curves for ^{6}Be are shifted to higher excitation energies in comparison to ^{6}He. However, if we compare *excitation energies* for peaks in IVSDM in ^{6}He and ^{6}Be they appear to be about the same (and even somewhat lower in ^{6}Be). At the moment we may point only to a qualitative agreement between our model calculations and different types of "soft" data, see Fig. 6.

(v) The proposed phenomenon is a "major effect". It can be easily seen in Fig. 2, that it responsible or the dominating part ($\sim 60\%$) of the cross section for population of ^{6}Be

states under ~ 16 MeV in the charge-exchange reaction. As dominating phenomenon, the IVSDM thus deserves a serious attention.

(vi) Specific profile of the IVSDM cross section depends on the details of the reaction mechanism. In particular, it sizably depends on the transferred momentum q. It means that attempts to characterize IVSDM in terms of states with definite energies and widths do not correspond to physics of the phenomenon. The title "excitation mode" characterises this phenomenon correctly: large observable effect, which is, however, sensitive to specific observation conditions.

8. Experimental discussion of IVSDM energy range

The charge-exchange (p, n) or $(^3\text{He}, t)$ reactions populating the ^{6}Be continuum have been studied several times within last four decades. However, the standard compilation [26] shows a "desert" in the excitation spectrum of ^{6}Be from 1.67 to 23 MeV indicating a very uncertain situation.

Older studies [27, 28, 5, and Refs. therein] were confined to narrow angular ranges of ^{6}Be c.m. ("point-like kinematics"). For certain angular ranges, the excitation spectra similar to ours have been obtained in Refs. [19, 5]. In all these cases, the spin-parity identification was not possible and the excitations above 2^+ state have been interpreted as three-body $\alpha + p + p$ phase volume.

In paper [12], the ^{6}Be spectrum was populated by using (p, n) reaction with a higher energy beam (186 MeV protons). Above the 2^+ state of ^{6}Be, four groups of events with important $\Delta L = 1$ component were distinguished at $E^* \sim 5.5, 10, 15$, and 25 MeV . According to interpretation of Ref. [12], the cross section in the range $E^* \sim 3 - 16$ MeV has significant contribution of $\Delta L = 0$ (from about 50% at $E^* \sim 3$ MeV to zero at $E^* \sim 12$ MeV) and important quasifree contribution (from 20% at $E^* \sim 3$ MeV to about 60% at $E^* \sim 16$ MeV). Total contribution of $\Delta L = 1$ can be estimated as $\sim 40\%$ in average in the whole range $E^* \sim 3 - 16$ MeV in this interpretation. In contrast, we do not see separate groups of events in the range $E^* \sim 3 - 16$ MeV; our spectrum is very smooth and has superb statistics. Our data do not allow a sizable contribution of $\Delta L = 0$ in the range $E^* \sim 3 - 16$ MeV. Our data also do not allow a sizable contribution of uncorrelated background in the range $E^* \sim 3 - 16$ MeV.

Isovector dipole strength has been considered in the studies of "mirror" ^{6}Li($^AZ, ^AZ+1$)^{6}He reactions [9, 29, 10, 11]. Two most recent works provide quality data and complicated interpretation. Our theoretical results indicate very similar pictures for IVSDM populating ^{6}He and ^{6}Be continuum enabling us to speculate about IVSDM in ^{6}He on the basis of our data. We see a considerably different interpretation for the ^{6}He data of Refs. [10, 11].

According to paper [10], the broad structure at $E^* = 4 - 15$ MeV consists of (i) "dipole excitation mode" at ~ 4 MeV with $\Delta S = 1$, (ii) "low-energy wing" of GDR at ~ 8.5 MeV formed by a $\Delta S = 0$ transition, and (iii) "spin dipole resonance" at ~ 8.5 MeV with $\Delta S = 1$ which was assumed to have the same profile as GDR. This work used γ-coincidences to distinguish $\Delta S = 0, 1$ contributions. However, the measurements were confined to extreme for-
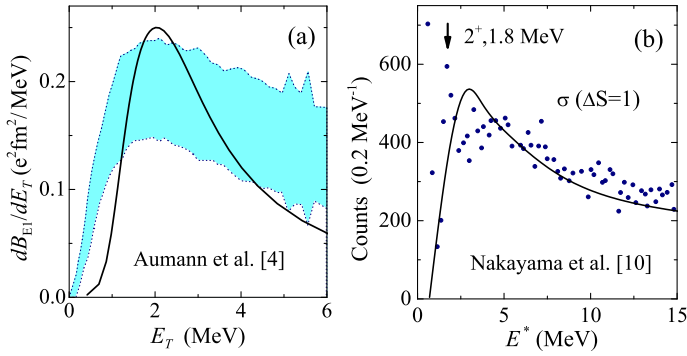
Fig. 6. Qualitative comparison (a) of SDM calculations (solid curve) with ^{6}He data [4] (blue shaded range), and (b) IVSDM calculations (solid curve) with ^{6}He data [10] (diamonds).

ward angles ($\sim 2°$) providing very limited ground for separation of contributions with different ΔL. Conclusions of paper [10] that "dipole excitation mode" peak has higher energy than in the works [4, 23] gets natural explanation in our results comparing SDM and IVSDM, see Fig. 3. We can not separate "dipole excitation mode" and "spin dipole resonance" (in terms of [10]) in the calculations with $\Delta S = 1$: there is no specific physical mechanism or quantum number selectivity in this energy range. However, the calculations with ingredients providing the low-energy peak in electromagnetic transition [Fig. 6 (a)], reproduce well the broad profile of cross section from [10] in the case of charge-exchange transition [Fig. 6 (b)]. Therefore, we find it reasonable to interpret the continuum from 4 to 15 MeV of excitation in ^{6}He as one structure defined by the same phenomenon.

Two broad structures populated by $\Delta L = 1$ in the ^{6}Li(T,^{3}He)^{6}He reaction were found in Ref. [11]: at $E^* \sim 5$ MeV (decomposed into 4.4, 7.7, and 9.9 MeV peaks) and at $E^* \sim 15$ MeV. According to the interpretation of this work, a "semi-phenomenological parameterisation of quasi-free scattering" contributes a lot (more than 50% at $E^* \sim 10$ MeV). The $E^* \sim 5$ MeV structure is interpreted as being composed of intruder states indicating quenching of the $1p$-$2s$ shell gap in ^{6}He. In our work, the correlation patterns in Fig. 4 exclude a possibility of some sizable phase-volume-like "background". The simple dynamic mechanism of the IVSDM population described by Eqs. (3,4) does not require intruder states (s-wave motion in the system is nonresonant) and does not imply any shell gap quenching.

Concluding the discussion of the previous observations, our interpretation is different and significantly clarify the situation with the "soft" excitations in $A = 6$ nuclei. It can be seen in Figs. 2 and 6, that our calculations provide very reasonable and consistent description of the three different sets of data: SDM in ^{6}He, IVSDM in ^{6}He and ^{6}Be branches.

9. Conclusion

High-statistics data on ^{6}Be continuum was obtained in the charge-exchange $p(^6$Li,^{6}Be)n reaction. The spectrum up to 16 MeV of energy E_T is completely described by population of three main structures in ^{6}Be: 0^+ at 1.37 MeV, 2^+ at 3.05 MeV, and the $\{0^-, 1^-, 2^-\}$ continuum state mixture

at $\sim 4 - 16$ MeV. The negative parity continuum is interpreted as a novel phenomenon — isovector soft dipole mode — presumably bringing new opportunities in the nuclear structure studies.

REFERENCES

1. K. Ikeda, INS Report JHP-7, in Japanese (1988).
2. P. Hansen, B. Jonson, Europhys. Lett. 4 (1987) 409.
3. C. Bertulani, G. Baur, Nucl. Phys. **A480** (1988) 615.
4. T. Aumann, Eur. Phys. J. A **26** (2005) 441.
5. O. Bochkarev *et al.*, Sov. J. Nucl. Phys. **55** (1992) 955.
6. V.I. Goldansky, Nucl. Phys. **19** (1960) 482.
7. L.V. Grigorenko *et al.*, Phys. Lett. **B677** (2009) 30.
8. L.V. Grigorenko *et al.*, Phys. Rev. C **80** (2009) 034602.
9. S. Sakuta *et al.*, Europhys. Lett. **22** (1993) 511.
10. S. Nakayama *et al.*, Phys. Rev. Lett. **85** (2000) 262.
11. T. Nakamura, Eur. Phys. J. A **13** (2002) 33.
12. X. Yang *et al.*, Phys. Rev. C **52** (1995) 2535.
13. http://flerovlab.jinr.ru/flnr/u400m.html
14. A.M. Rodin *et al.*, Nucl. Instr. Meth. **A391** (1997) 228.
15. B. Danilin *et al.*, Phys. Rev. C **43** (1991) 2835.
16. L.V. Grigorenko, K. Langanke, N.B. Shul'gina, M.V. Zhukov, Phys. Lett. **B641** (2006) 254.
17. M. S. Golovkov *et al.*, Phys. Lett. **B672** (2009) 22.
18. H. Esbensen, G.F. Bertsch, Nucl. Phys. **A542** (1992) 310.
19. C. Batty *et al.*, Nucl. Phys. **A120** (1968) 297.
20. J. Rapaport *et al.*, Phys. Rev. C **41** (1990) 1920.
21. F. Petrovich *et al.*, Nucl. Phys. **A563** (1993) 387.
22. A. Cobis, D. Fedorov, A. Jensen, Phys. Rev. Lett. **79** (1997) 2411.
23. B. Danilin, I. Thompson, J. Vaagen, M. Zhukov, Nucl. Phys. **A632** (1998) 383.
24. T. Myo, K. Kato, S. Aoyama, K. Ikeda, Phys. Rev. C **63** (2001) 054313.
25. B.L. Berman, S.C. Fultz, Rev. Mod. Phys. **47** (1975) 713.
26. D. Tilley *et al.*, Nucl. Phys. **A708** (2002) 3.
27. R. Givens, M. Brussel, A. Yavin, Nucl. Phys. **A187** (1972) 490.
28. D.F. Geesaman *et al.*, Phys. Rev. C **15** (1977) 1835.
29. J. Jänecke *et al.*, Nucl. Phys. **A599** (1996) 191c.